



Application of Chest CT Imaging Feature Model in Distinguishing Squamous Cell Carcinoma and Adenocarcinoma of the Lung

Chunmei Liu ¹, Yuzheng He ², Jianmin Luo ³

¹Department of Radiation Oncology, The Second Hospital of Hebei Medical University, Shijiazhuang, Hebei Province, People's Republic of China;

²Department of Thoracic Surgery, The Second Hospital of Hebei Medical University, Shijiazhuang, Hebei Province, People's Republic of China;

³Department of Hematology, The Second Hospital of Hebei Medical University, Shijiazhuang, Hebei Province, People's Republic of China

Correspondence: Jianmin Luo, Department of Hematology, The Second Hospital of Hebei Medical University, 215 West Heping Road, Shijiazhuang, Hebei Province, People's Republic of China, Tel +86 1348368527, Email luojm31555@163.com

Purpose: In situations where pathological acquisition is difficult, there is a lack of consensus on distinguishing between adenocarcinoma and squamous cell carcinoma from imaging images, and each doctor can only make judgments based on their own experience. This study aims to extract imaging features of chest CT, extract sensitive factors through logistic univariate and multivariate analysis, and model to distinguish between lung squamous cell carcinoma and lung adenocarcinoma.

Methods: We downloaded chest CT scans with clear diagnosis of adenocarcinoma and squamous cell carcinoma from The Cancer Imaging Archive (TCIA), extracted 19 imaging features by a radiologist and a thoracic surgeon, including location, spicule, lobulation, cavity, vacuolar sign, necrosis, pleural traction sign, vascular bundle sign, air bronchogram sign, calcification, enhancement degree, distance from pulmonary hilum, atelectasis, pulmonary hilum and bronchial lymph nodes, mediastinal lymph nodes, interlobular septal thickening, pulmonary metastasis, adjacent structures invasion, pleural effusion. Firstly, we apply the glm function of R language to perform logistic univariate analysis on all variables to select variables with $P < 0.1$. Then, perform logistic multivariate analysis on the selected variables to obtain a predictive model. Next, use the roc function in R language to calculate the AUC value and draw the ROC curve, use the val.prob function in R language to draw the Calibrat curve, and use the rmda package in R language to draw the DCA curve and clinical impact curve. At the same time, 45 patients diagnosed with lung squamous cell carcinoma and lung adenocarcinoma through surgery or biopsy in the Radiotherapy Department and Thoracic Surgery Department of our hospital from 2023 to 2024 were included in the validation group. The chest CT features were jointly determined and recorded by the two doctors mentioned above and included in the validation group. The included image feature data are complete and does not require preprocessing, so directly entering statistical calculations. Perform ROC curves, calibration curves, DCA, and clinical impact curves in the validation group to further validate the predictive model. If the predictive model performs well in the validation group, further draw a nomogram to demonstrate.

Results: This study extracted 19 imaging features from the chest CT scans of 75 patients downloaded from TCIA and finally selected 18 complete data for analysis. First, univariate analysis and multivariate analysis were performed, and a total of 5 variables were obtained: spicule, necrosis, air bronchogram Sign, atelectasis, pulmonary hilum and bronchial lymph nodes. After conducting modeling analysis with $AUC = 0.887$, a validation group was established using clinical cases from our hospital, Draw ROC curve with $AUC = 0.865$ in the validation group, evaluate the accuracy of the model through Calibrate calibration curve, evaluate the reliability of the model in clinical practice through DCA curve, and further evaluate the practicality of the model in clinical practice through clinical impact curve.

Conclusion: It is possible to extract influential features from ordinary chest CT scans to determine lung adenocarcinoma and squamous cell carcinoma. The model we have set up performs well in terms of discrimination, accuracy, reliability, and practicality.

Keywords: lung cancer, LUAD, LSCC, image features, predict

Introduction

The pathology of lung cancer is very important in personalized and precise treatment,^{1,2} but in clinical practice, we inevitably encounter a challenge, which is that sometimes only a small number of tumor cells can be found after biopsy, and even necrotic cells can only be seen. Even after immunohistochemistry, the specific pathological type cannot be

determined. Based on tumor markers, we can sometimes further rule out the diagnosis of small cell lung cancer, but further distinguishing between squamous cell carcinoma and adenocarcinoma is basically impossible. Pathological patients who undergo biopsy again often refuse due to risk and pain. But there are significant differences in treatment options between squamous cell carcinoma and adenocarcinoma, according to the National Comprehensive Cancer Network (NCCN) guidelines.³ At this point, doctors have no other choice but to make further judgments based on imaging features. However, this judgment requires rich clinical experience and a high error rate. This leads to a lack of precise treatment for patients with unclear pathology, resulting in a decrease in treatment effectiveness and a shortened survival time. Therefore, how to distinguish lung squamous cell carcinoma and adenocarcinoma based on common chest CT imaging features has become a challenge in treating patients with unclear pathology.

Some studies have also attempted to model by extracting features from various image data, some based on CT texture features,^{4,5,6} some based on the iodine concentration of enhanced CT,⁷ some rely on the attenuation rate of enhanced CT,⁸ some models are established based on the perfusion parameters of brain metastases,⁹ some use PET-CT,^{10,11} and some combine machine learning.^{12–16} However, these examinations increase the economic burden on patients or are difficult to operate, and they have not been proven to be clinically applicable. Because chest CT scans are more common and cost-effective, it is more meaningful and beneficial for patients to distinguish between adenocarcinoma and squamous cell carcinoma based on chest CT scans. In the past, only one study based on chest CT features studied the pathological differences of lung cancer,¹⁷ but he did not further analyze the differences between squamous cell carcinoma and adenocarcinoma. This study aims to extract traditional imaging features from chest CT plain scans and analyze them, aiming to obtain a reliable predictive model to help clinical doctors distinguish between lung squamous cell carcinoma and lung adenocarcinoma.

Method

Download images with squamous cell carcinoma or adenocarcinoma from The Cancer Imaging Archive (TCIA). Inclusion criteria: 1. Pathologically confirmed as lung squamous cell carcinoma or lung adenocarcinoma; 2. The contour of lung tumors is relatively clear; 3. Complete lung tumor scanning; 4. CT is a plain or enhanced image. Exclusion criteria: 1. Unclear pathology; 2. A large amount of pleural effusion or pneumonia obstructs the contour of the tumor; 3. Incomplete lung tumor scanning; 4. Identify cases with significant tumor changes after radiotherapy or chemotherapy. A radiologist and a thoracic surgeon jointly determined 19 chest CT features, including location, spicule, lobulation, cavity, vacuolar sign, necrosis, pleural traction sign, vascular bundle sign, air bronchogram sign, calcification, enhancement degree, distance from pulmonary hilum, atelectasis, pulmonary hilum and bronchial lymph nodes, mediastinal lymph nodes, interlobular septal thickening, pulmonary metastasis, adjacent structures invasion, pleural effusion, pathology and record, enter the training group. If there is a lot of missing data in the feature, it will be removed. Firstly, we apply the glm function of R language to perform logistic univariate analysis on all variables to select variables with $P < 0.1$. Then, perform logistic multivariate analysis on the selected variables to obtain a predictive model. Next, use the roc function in R language to calculate the AUC value and draw the ROC curve, use the val.prob function in R language to draw the Calibrat curve, use the rmda package in R language to draw the DCA curve and clinical impact curve. At the same time, 45 patients diagnosed with lung squamous cell carcinoma and lung adenocarcinoma through surgery or biopsy in the Radiotherapy Department and Thoracic Surgery Department of our hospital from 2023 to 2024 were included. The chest CT features were jointly determined and recorded by the two doctors mentioned above and included in the validation group. The included image feature data is complete and does not require preprocessing, so directly entering statistical calculations. Perform ROC curves, calibration curves, DCA, and clinical impact curves in the validation group to further validate the predictive model. If the predictive model performs well in the validation group, further draw a nomogram to demonstrate.

Result

Univariate Analysis of Training Group

Chest CT scans of 75 patients diagnosed with adenocarcinoma and squamous cell carcinoma were downloaded from The Cancer Imaging Archive (TCIA). They will be included in the training group (CMB-LCA, CPTAC-LUAD, CPTAC-LSCC),^{18–20} After sorting out its 19 image features, it was found that the degree of enhancement was missing by 30%, so

it was removed. Therefore, the actual image features that entered the analysis were 18, which including location, spicule, lobulation, cavity, vacuolar sign, necrosis, pleural traction sign, vascular bundle sign, air bronchogram sign, calcification, distance from pulmonary hilum, atelectasis, pulmonary hilum and bronchial lymph nodes, mediastinal lymph nodes, interlobular septal thickening, pulmonary metastasis, adjacent structures invasion, pleural effusion. The glm package of R language was applied for logistic univariate analysis, and the results are shown in Table 1. Further extract features with $P < 0.05$ and $P < 0.1$ as follows: spicule, necrosis, air bronchogram sign, atelectasis, pulmonary hilum and bronchial lymph nodes (Table 2) and spicule, necrosis, pleural traction sign, air bronchogram sign, atelectasis, pulmonary hilum and bronchial lymph nodes (Table 3). Select variables with $P < 0.1$ for the next step of multi factor analysis.

Multivariate Analysis of Training Group

Selecting variables with univariate analysis result $P < 0.1$, and conducting multiple factor regression analysis using enter, forward, back, and both methods, it was found that the AIC values for forward, back, and both were the same, with AIC = 73.66533, which was lower than the AIC value of the enter method. Therefore, both stepwise regression method was selected for multivariate analysis, and the results are shown in Table 4. The final image features that enter modeling are spicule, necrosis, air bronchogram sign, atelectasis, pulmonary hilum and bronchial lymph nodes.

ROC Curves for Training Groups

We use ROC curves for model discrimination evaluation in training groups. First, draw the ROC curve in the training group with AUC = 0.887 and 95% confidence interval of 0.812–0.963, as shown in Figure 1.

Table 1 Results of Logistic Univariate Analysis

Characteristics	B	SE	OR	CI	Z	P
Location	-0.065	0.18	0.94	0.66–1.33	-0.361	0.718
Spicule	-1.158	0.333	0.31	0.16–0.6	-3.478	0.001
Lobulation	-0.584	0.802	0.56	0.12–2.69	-0.728	0.467
Cavity	17.972	1769.258	63,817,219	0-Inf	0.01	0.992
Vesicles	-1.003	0.713	0.37	0.09–1.48	-1.408	0.159
Necrosis	0.999	0.481	2.71	1.06–6.97	2.077	0.038
Pleuraltraction	-0.875	0.479	0.42	0.16–1.07	-1.828	0.068
Vascular	-0.468	0.572	0.63	0.2–1.92	-0.819	0.413
Airbron	-1.121	0.491	0.33	0.12–0.85	-2.284	0.022
Calcification	-0.241	0.233	NA	NA-NA	-1.037	0.3
Distance	-0.096	0.093	0.91	0.76–1.09	-1.029	0.304
Atelectasis	1.872	0.704	6.5	1.64–25.83	2.66	0.008
Hilarlym	1.821	0.635	6.17	1.78–21.44	2.867	0.004
Mediastinallym	0.949	0.852	2.58	0.49–13.72	1.113	0.266
Interlobular	-0.464	0.476	0.63	0.25–1.6	-0.976	0.329
Metastasis	0.27	0.749	1.31	0.3–5.69	0.361	0.718
Invasion	-0.276	0.625	0.76	0.22–2.58	-0.442	0.659
Hydrothorax	-0.47	1.247	0.63	0.05–7.2	-0.377	0.706

Table 2 Image Characteristics with $P < 0.05$

Characteristics	B	SE	OR	CI	Z	P
Spicule	-1.158	0.333	0.31	0.16–0.6	-3.478	0.001
Necrosis	0.999	0.481	2.71	1.06–6.97	2.077	0.038
Airbron	-1.121	0.491	0.33	0.12–0.85	-2.284	0.022
Atelectasis	1.872	0.704	6.5	1.64–25.83	2.66	0.008
Hilarlym	1.821	0.635	6.17	1.78–21.44	2.867	0.004

Table 3 Image Characteristics with P<0.1

Characteristics	B	SE	OR	CI	Z	P
Spicule	-1.158	0.333	0.31	0.16-0.6	-3.478	0.001
Necrosis	0.999	0.481	2.71	1.06-6.97	2.077	0.038
Pleuraltraction	-0.875	0.479	0.42	0.16-1.07	-1.828	0.068
Airbron	-1.121	0.491	0.33	0.12-0.85	-2.284	0.022
Atelectasis	1.872	0.704	6.5	1.64-25.83	2.66	0.008
Hilarlym	1.821	0.635	6.17	1.78-21.44	2.867	0.004

Table 4 Results of Logistic Multivariate Analysis

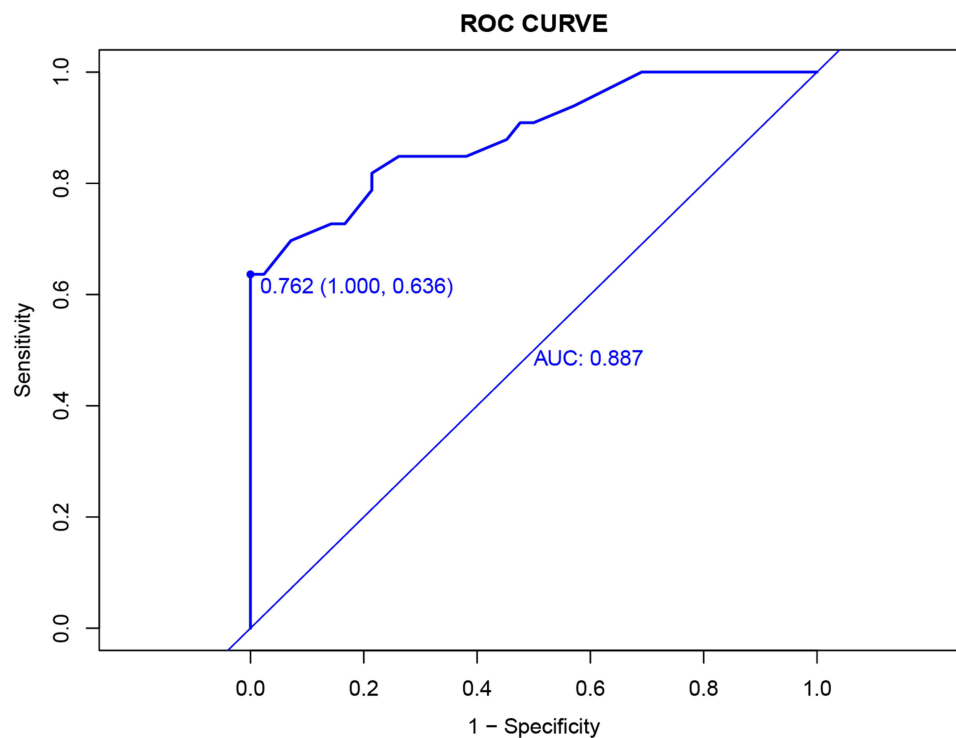
Characteristics	B	SE	OR	CI	Z	P
Spicule	-1.368	0.446	0.25	0.11-0.61	-3.065	0.002
Necrosis	1.209	0.661	3.35	0.92-12.24	1.829	0.067
Airbron	-1.312	0.695	0.27	0.07-1.05	-1.888	0.059
Atelectasis	2.42	0.91	11.25	1.89-66.93	2.66	0.008
Hilarlym	2.865	0.898	17.56	3.02-102.05	3.19	0.001

Calibrate Validation Curves for Training Groups

We use the Calibrate curve to evaluate the accuracy of the model. First, draw the Calibrate curve (Figure 2) in the training group, which shows $p = 0.956$, showing that the accuracy of the model is extremely high.

DCA curves and confidence intervals for training groups

We use DCA curves to evaluate the reliability of the model in clinical practice. Draw the DCA curve and confidence interval (Figure 3A and B) in the training group using the RMDA package of R language, and search for literature^{21,22} to

**Figure 1** Training group ROC curve.

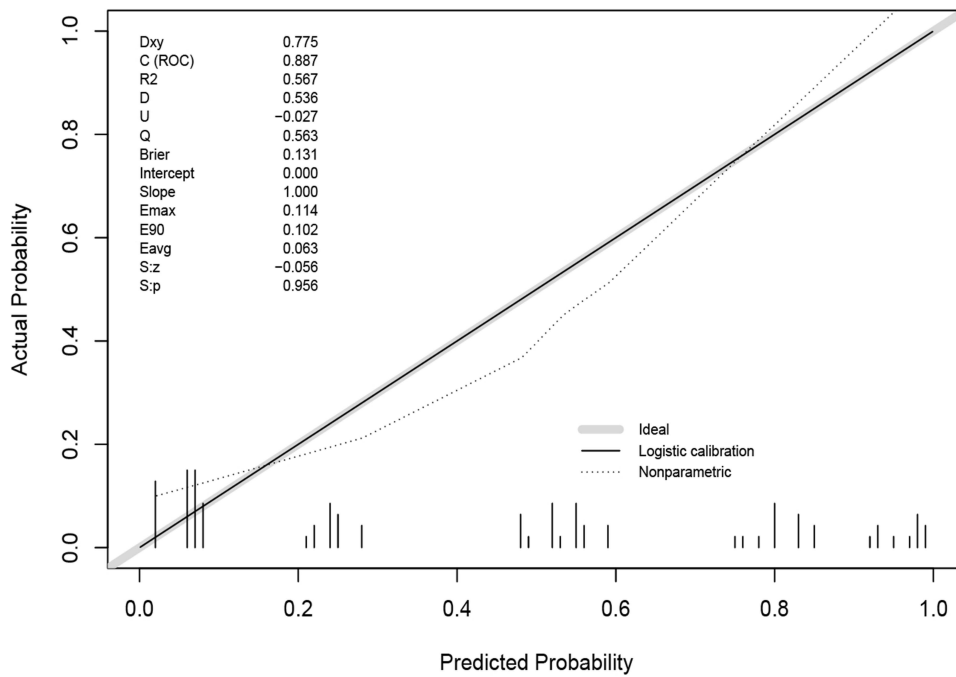


Figure 2 Training group Calibrate curve.

determine a 20% incidence rate for squamous cell carcinoma and an 80% incidence rate for adenocarcinoma. Therefore, setting the parameter population validity = 0.2 shows good reliability.

ROC Curves for Validation Groups

We use ROC curves for model discrimination evaluation in validation groups. We use R language to draw the ROC curve in the validation group with AUC = 0.865 and 95% confidence interval of 0.756–0.975, as shown in Figure 4.

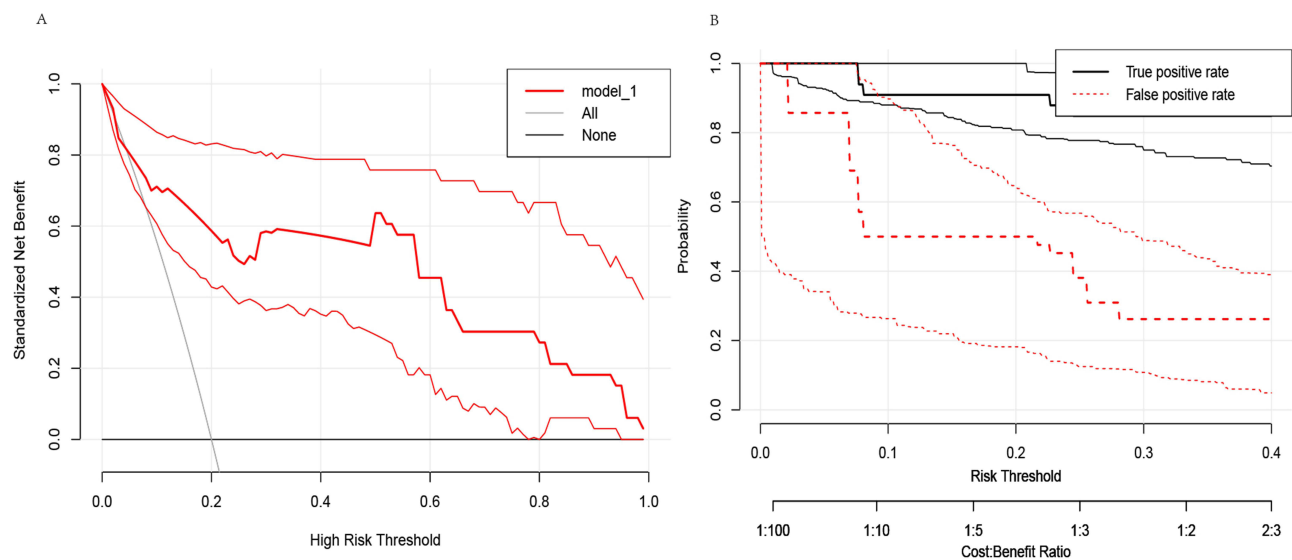


Figure 3 (A). Training group DCA curve. (B). confidence interval.

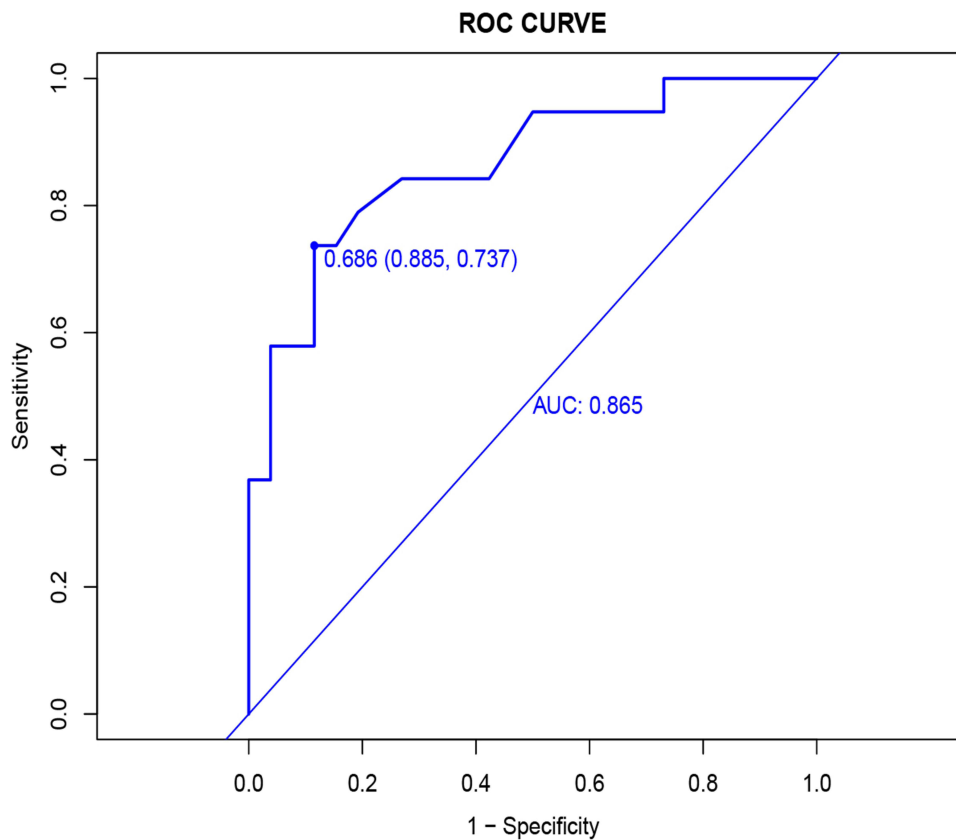


Figure 4 Validation group ROC curve.

Calibrate Validation Curves for Validation Groups

We use the Calibrate curve to evaluate the accuracy of the model in validation groups. Using R language to draw a Calibrate curve (Figure 5) in the validation group, with $P = 0.179$. The accuracy of the model was not as good as in the training group, but the P value was greater than 0.05, showing good accuracy.

DCA Curves and Confidence Intervals for Validation Groups

We use DCA curves to evaluate the reliability of the model in clinical practice in validation groups. First, set the parameter population validity = 0.2. Then, in the validation group, a DCA curve and confidence interval (Figure 6A and B) were plotted, and the results showed that reliability was not as good as in the training group.

Clinical Impact Curve

We further evaluate the practicality of the model in clinical practice using clinical impact curves. By using the RMDA package in R language to draw a clinical impact curve (Figure 7), it can be seen that the solid red line is very close to the solid blue line, indicating good reliability of the model.

Nomogram Column Chart

Finally, we visualize the established model and use the rms package in R language to draw a Nomogram column chart (Figure 8).

Discussion

For patients who are difficult to undergo surgery or biopsy, or whose pathology cannot be decided after biopsy, distinguishing between lung squamous cell carcinoma and adenocarcinoma is a widespread problem that troubles clinical

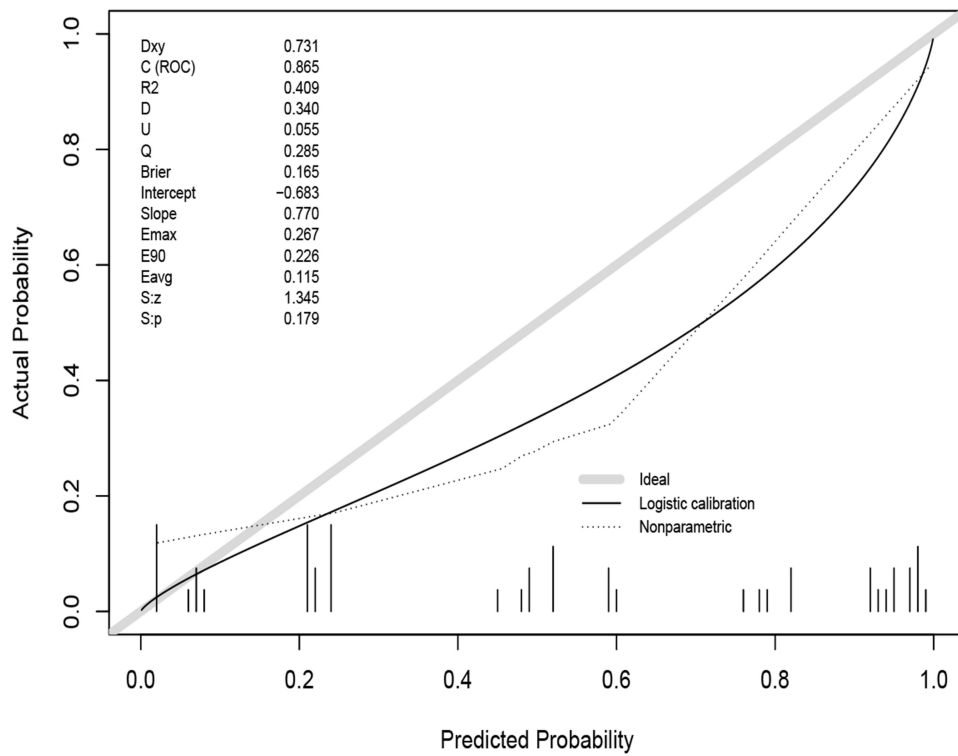


Figure 5 Validation group Calibrate curve.

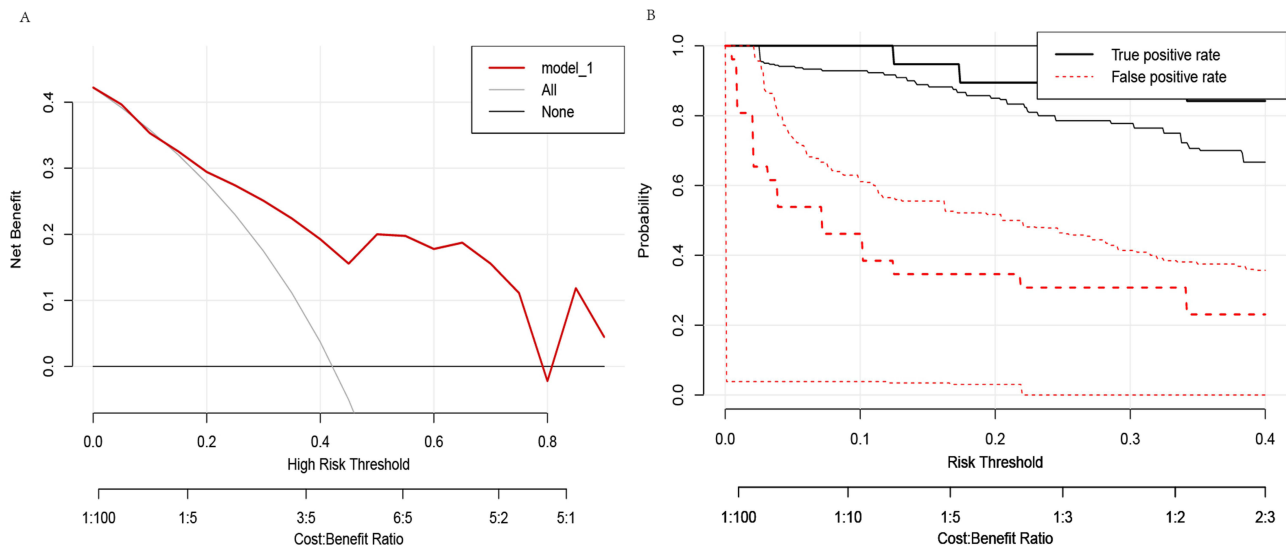


Figure 6 (A) Verification group DCA curve. (B) confidence interval.

doctors, and there is currently no good method. This study extracted image features from chest CT downloaded from TCIA and conducted modeling analysis with AUC = 0.887. A validation group was set up using clinical cases from our hospital, and an ROC curve with AUC = 0.865 was drawn in the validation group. The accuracy of the model was evaluated through the Calibration curve, the reliability of the model in clinical practice was evaluated through the DCA curve, and the clinical impact curve was further evaluated to evaluate the practicality of the model in clinical practice. Prove that the model has certain clinical application value.

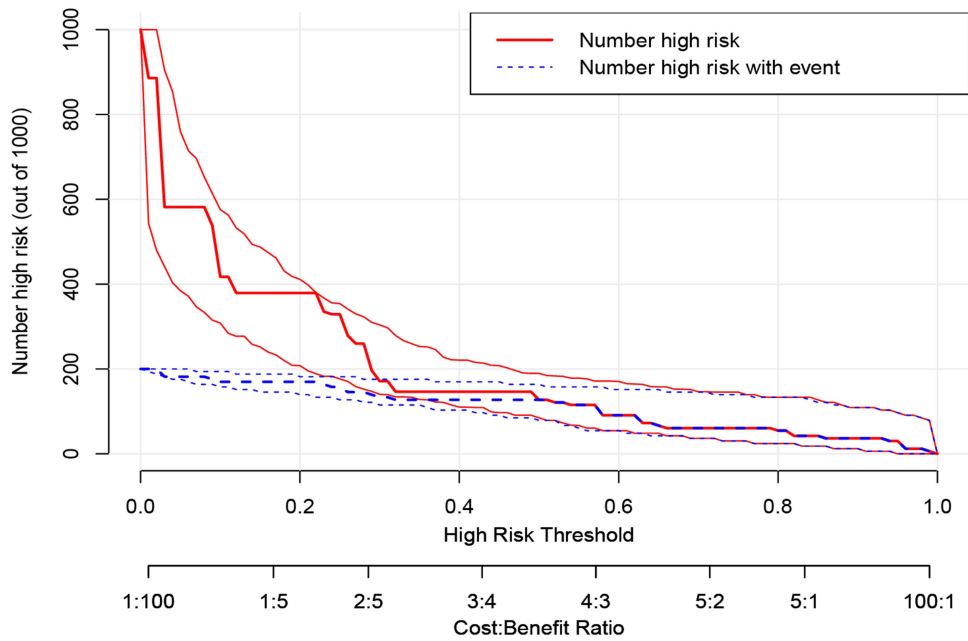


Figure 7 Clinical impact curve.

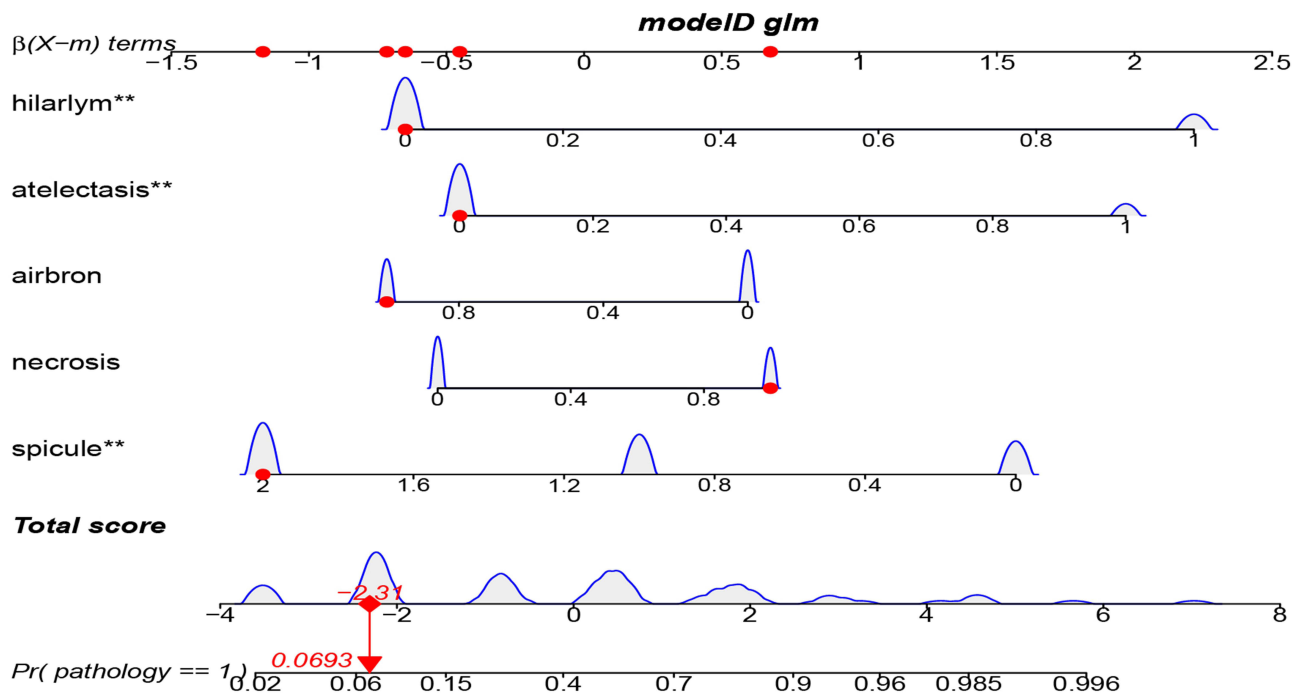


Figure 8 Nomo column chart.

There have been many literature reports on the application of imaging features for pathological prediction in the past.^{5-13,17,23-33} Han et al found that a model for distinguishing lung squamous cell carcinoma and lung adenocarcinoma was constructed using CT texture features, with an AUC of 0.803,⁵ Zhang et al established a model based on the variation of iodine concentration in enhanced CT, with an AUC of 0.871,⁷ Fukuma et al established a model based on the attenuation rate of enhanced CT, with an AUC of only 0.625,⁸ Jiang et al established a model based on the perfusion parameters of brain metastases, with an AUC of 0.845,⁹ Tomori et al established a model using a combination of PET-CT

and CT imaging features, with an AUC of 0.92,¹¹ Lin et al combined machine learning to establish a model with a maximum AUC 0.8,¹² Tang et al combined machine learning to establish a model with a maximum AUC 0.87,¹³ But these examinations will increase the financial burden on patients, and some patients with allergic constitution are not suitable for enhanced examinations, while ordinary chest CT plain scans are more common and economical. Yue et al²⁴ found that the imaging features of chest CT are a fast and widely available way to distinguish between lung squamous cell carcinoma and adenocarcinoma. However, these articles usually require the use of radiomics to extract data features from images in order to make judgments, and this process requires complex computer technologies such as image segmentation and Python software operation, which is still very difficult for clinical doctors. Therefore, I conducted a literature search based on how to apply chest CT to distinguish adenocarcinoma and squamous cell carcinoma. I did not find any research on using the imaging features of chest CT for modeling to help distinguish between lung squamous cell carcinoma and adenocarcinoma. This study downloaded chest CT from the TCIA database, reducing human intervention in cases and setting up a model for predicting lung adenocarcinoma and squamous cell carcinoma with AUC = 0.887. The AUC of the models developed in the above studies is 0.625 for the lowest, 0.92 for the highest, and mostly 0.8. The AUC of this study is 0.887, which belongs to the upper moderate level. Moreover, the data source of this study is the most ordinary chest CT, so the results of this study are reliable and practical.

This study has some limitations. Firstly, the number of cases is relatively small, which to some extent reduces the applicability of the model. Secondly, due to the high number of cases with enhanced CT, there is a lack of enhancement factors. Also, due to the selection of multiple influencing features in this study, no identical or similar articles were found, so it was not possible to compare the ROC with other articles. Finally, using chest CT alone to determine lung adenocarcinoma and squamous cell carcinoma itself has significant limitations. This study intends to analyze this only because it has found that many medical colleagues are interested in using chest CT to determine pathological subtypes and have engaged in heated discussions. However, there is no consensus. The image features adopted in this study are the basis mentioned by doctors on the Chinese Internet during their discussion. It is hoped that this study can also provide some judgmental basis for doctors. However, due to the small sample size of this study, it may result in biased results. Therefore, the five features proposed in this article require further clinical validation and future research improvements with larger sample sizes. Clinicians can strengthen the weights of five features, including spicule, necrosis, air bronchogram sign, atelectasis, pulmonary hilum and bronchial lymph nodes when using their own experience to make judgments, with a basis to preliminarily distinguish between lung squamous cell carcinoma and lung adenocarcinoma, and make personalized treatment choices with more confidence in treatment. In the future, we will accumulate more cases to enrich the research sample of this experiment, so as to make the results closer to the real world and improve the accuracy of evaluation.

Conclusion

It is currently very difficult to distinguish between lung adenocarcinoma and lung squamous cell carcinoma in clinical practice when pathology is difficult to obtain. Our study found that extracting specific features from regular chest CT scans is feasible for identifying lung adenocarcinoma and squamous cell carcinoma. The model we have established performs well in terms of discrimination, accuracy, reliability, and practicality. This provides more evidence for ordinary clinical doctors to distinguish between squamous cell carcinoma and adenocarcinoma, which is more reliable than relying solely on personal experience. In the future, we need more cases to improve the model.

Data Sharing Statement

The datasets generated during and/or analyzed during the current study are not publicly available due to privacy of patient information but are definitely available from the corresponding author if requested. All requests are greeted.

Ethics Declarations and Consent to Participate

This retrospective study was carried out using the opt-out method for the case series of our hospital. The study was approved by the Research Ethics Committee of the second hospital of Hebei Medical University (approval no 2024-R019) and was conducted in accordance with the 1964 Helsinki Declaration and its later amendments or comparable

ethical standards. Informed consent was waived by the Research Ethics Committee of the second hospital of Hebei Medical University due to the retrospective nature of the study, and all clinical data was anonymized during analysis to maintain the patient privacy. And all methods were performed in accordance with the relevant guidelines and regulations of the committee of The Second Hospital of Hebei Medical University.

Author Contributions

Chunmei Liu wrote the manuscript and all the figures, downloaded imaging, and read image features, Yuzheng He jointly analyze image data and extract image features, Jianmin Luo design the study. All authors made a significant contribution to the work reported, whether that is in the conception, study design, execution, acquisition of data, analysis and interpretation, or in all these areas; took part in drafting, revising or critically reviewing the article; gave final approval of the version to be published; have agreed on the journal to which the article has been submitted; and agree to be accountable for all aspects of the work.

Funding

This work was supported by the Health of Hebei Province Commission for medical scientific research funding of China (No. 20180396).

Disclosure

The authors declare that there is no conflict of interests.

References

1. Lee Y, Lee B, Choi YL, Kang DW, Han J. Clinicopathologic and molecular characteristics of HER2 (ERBB2)-altered non-small cell lung cancer: implications for precision medicine. *Mod Pathol.* 2024;37:100490. doi:10.1016/j.modpat.2024.100490
2. Bertolaccini L, Casiraghi M, Uslenghi C, Maiorca S, Spaggiari L. Recent advances in lung cancer research: unravelling the future of treatment. *Updates Surg.* 2024. doi:10.1007/s13304-024-01841-3
3. The National Comprehensive Cancer Network. Non-small cell lung cancer; 2024. Available from: <https://www.nccn.org/guidelines/guidelines-detail?category=1&id=1450>. Accessed May 28, 2024.
4. Liu H, Jing B, Han W, Long Z, Mo X, Li H. A comparative texture analysis based on NECT and CECT images to differentiate lung adenocarcinoma from squamous cell carcinoma. *J Med Syst.* 2019;43(3):59. doi:10.1007/s10916-019-1175-y
5. Han R, Arjal R, Dong J, et al. Three dimensional texture analysis of noncontrast chest CT in differentiating solitary solid lung squamous cell carcinoma from adenocarcinoma and correlation to immunohistochemical markers. *Thoracic Cancer.* 2020;11(11):3099–3106. doi:10.1111/1759-7714.13592
6. Fried DV, Tucker SL, Zhou S, et al. Prognostic value and reproducibility of pretreatment CT texture features in stage III non-small cell lung cancer. *Int J Radiat Oncol Biol Phys.* 2014;90(4):834–842. doi:10.1016/j.ijrobp.2014.07.020
7. Zhang Z, Zou H, Yuan A, et al. A single enhanced dual-energy CT Scan may distinguish lung squamous cell carcinoma from adenocarcinoma during the venous phase. *Acad Radiol.* 2020;27(5):624–629. doi:10.1016/j.acra.2019.07.018
8. Fukuma S, Shinya T, Soh J, et al. Association between Histological Types and Enhancement of Dynamic CT for Primary Lung Cancer. *Acta medica Okayama.* 2020;74(2):129–135. doi:10.18926/AMO/58271
9. Jiang C, Liu X, Qu Q, Jiang Z, Wang Y. Prediction of adenocarcinoma and squamous carcinoma based on CT perfusion parameters of brain metastases from lung cancer: a pilot study. *Front Oncol.* 2023;13:1225170. doi:10.3389/fonc.2023.1225170
10. Aydos U, Ünal ER, Özçelik M, et al. Características de textura del tumor primario en imágenes de ¹⁸F-FDG PET en cáncer de pulmón de células no pequeñas: la relación entre parámetros de imágenes y parámetros histopatológicos. *Revista Espa De Med Nucl E Imag Molecul.* 2021;40(6):343–350. doi:10.1016/j.remna.2020.06.025
11. Tomori Y, Yamashiro T, Tomita H, et al. CT radiomics analysis of lung cancers: differentiation of squamous cell carcinoma from adenocarcinoma, a correlative study with FDG uptake. *Eur J Radiol.* 2020;128:109032. doi:10.1016/j.ejrad.2020.109032
12. Lin J, Yu Y, Zhang X, Wang Z, Li S. Classification of histological types and stages in non-small cell lung cancer using radiomic features based on CT images. *J Digit Imag.* 2023;36(3):1029–1037. doi:10.1007/s10278-023-00792-2
13. Tang X, Huang H, Du P, Wang L, Yin H, Xu X. Intratumoral and peritumoral CT-based radiomics strategy reveals distinct subtypes of non-small-cell lung cancer. *J Cancer Res Clin Oncol.* 2022;148(9):2247–2260. doi:10.1007/s00432-022-04015-z
14. Wang C, Ma J, Shao J, et al. Non-invasive measurement using deep learning algorithm based on multi-source features fusion to predict PD-L1 expression and survival in NSCLC. *Front Immunol.* 2022;13:1.
15. Qiu Q, Xing L, Wang Y, Feng A, Wen Q. Development and validation of a radiomics nomogram using computed tomography for differentiating immune checkpoint inhibitor-related pneumonitis from radiation pneumonitis for patients with non-small cell lung cancer. *Front Immunol.* 2022;2022:13.
16. Wen Q, Yang Z, Dai H, Feng A, Li Q. Radiomics study for predicting the expression of PD-L1 and tumor mutation burden in non-small cell lung cancer based on CT images and clinicopathological features. *Front Oncol.* 2021;11:620246. doi:10.3389/fonc.2021.620246

17. Ban X, Shen X, Hu H, et al. Predictive CT features for the diagnosis of primary pulmonary mucoid adenocarcinoma: comparison with squamous cell carcinomas and adenocarcinomas. *Cancer Imag.* 2021;21(1):2. doi:10.1186/s40644-020-00375-2
18. Cancer Moonshot Biobank. Cancer Moonshot Biobank – lung Cancer Collection (CMB-LCA) (Version 4) [dataset]. *Cancer Imaging Arch.* 2022. doi:10.7937/3CX3-S132
19. National Cancer Institute Clinical Proteomic Tumor Analysis Consortium (CPTAC). The clinical proteomic tumor analysis consortium lung squamous cell carcinoma collection (CPTAC-LSCC) (Version 14) [Data set]. *Cancer Imaging Arch.* 2018;2018:1. doi:10.7937/K9/TCIA.2018.6EMUB5L2
20. National Cancer Institute Clinical Proteomic Tumor Analysis Consortium (CPTAC). The clinical proteomic tumor analysis consortium lung adenocarcinoma collection (CPTAC-LUAD) (Version 12) [Data set]. *Cancer Imaging Arch.* 2018;2018:1. doi:10.7937/K9/TCIA.2018.PAT12TBS
21. of Committee LC. Chinese anti-cancer association LCSGoCoO, multicenter big data research project specialists of Chinese lung cancer. Current status of postoperative pathological diagnosis of lung cancer in China: a multicenter big data study. *Zhonghua bing li xue za zhi.* 2021;50(8):882–890. doi:10.3760/cma.j.cn112151-20210427-00328
22. Zhou Y, Xiang Z, Lin W, et al. Long-term trends of lung cancer incidence and survival in southeastern China, 2011–2020: a population-based study. *BMC Pulm Med.* 2024;24(1):25. doi:10.1186/s12890-024-02841-0
23. Khorrami M, Bera K, Leo P, et al. Stable and discriminating radiomic predictor of recurrence in early stage non-small cell lung cancer: multi-site study. *Lung Cancer.* 2020;142:90–97. doi:10.1016/j.lungcan.2020.02.018
24. Yue JY, Chen J, Zhou FM, et al. CT-pathologic correlation in lung adenocarcinoma and squamous cell carcinoma. *Medicine.* 2018;97(50):e13362. doi:10.1097/MD.00000000000013362
25. Yu L, Tao G, Zhu L, et al. Prediction of pathologic stage in non-small cell lung cancer using machine learning algorithm based on CT image feature analysis. *BMC Cancer.* 2019;19(1):464. doi:10.1186/s12885-019-5646-9
26. Ju H, Kim K, Kim BI, Woo S-K. Graph neural network model for prediction of non-small cell lung cancer lymph node metastasis using protein-protein interaction network and ¹⁸F-FDG PET/CT radiomics. *Int J Mol Sci.* 2024;25(2):698. doi:10.3390/ijms25020698
27. Li B, Su J, Liu K, Hu C. Deep learning radiomics model based on PET/CT predicts PD-L1 expression in non-small cell lung cancer. *Europ J Radiol Open.* 2024;12:100549. doi:10.1016/j.ejro.2024.100549
28. J-W M, Jiang X, Wang Y-M, et al. Dual-energy CT-based radiomics in predicting EGFR mutation status non-invasively in lung adenocarcinoma. *Heliyon.* 2024;10(2):e24372. doi:10.1016/j.heliyon.2024.e24372
29. Meng X, Xu H, Liang Y, et al. Enhanced CT-based radiomics model to predict natural killer cell infiltration and clinical prognosis in non-small cell lung cancer. *Front Immunol.* 2024;14:1334886. doi:10.3389/fimmu.2023.1334886
30. Zhang G, Man Q, Shang L, et al. Using multi-phase CT radiomics features to predict EGFR mutation status in lung adenocarcinoma patients. *Acad Radiol.* 2024;S1076-6332(23):1.
31. Zhang X, Zhang G, Qiu X, et al. Exploring non-invasive precision treatment in non-small cell lung cancer patients through deep learning radiomics across imaging features and molecular phenotypes. *Biomarker Res.* 2024;12(1):12. doi:10.1186/s40364-024-00561-5
32. Zuo Y, Liu L, Chang C, et al. Value of multi-center ¹⁸F-FDG PET/CT radiomics in predicting EGFR mutation status in lung adenocarcinoma. *Med Phys.* 2024. doi:10.1002/mp.16947
33. Zyla J, Marczyk M, Prazuch W, et al. Combining low-dose computer-tomography-based radiomics and serum metabolomics for diagnosis of malignant nodules in participants of lung cancer screening studies. *Biomolecules.* 2023;14(1):44. doi:10.3390/biom14010044

Cancer Management and Research

Dovepress

Publish your work in this journal

Cancer Management and Research is an international, peer-reviewed open access journal focusing on cancer research and the optimal use of preventative and integrated treatment interventions to achieve improved outcomes, enhanced survival and quality of life for the cancer patient. The manuscript management system is completely online and includes a very quick and fair peer-review system, which is all easy to use. Visit <http://www.dovepress.com/testimonials.php> to read real quotes from published authors.

Submit your manuscript here: <https://www.dovepress.com/cancer-management-and-research-journal>